ARMY RESEARCH LABORATORY

Directed Assembly of Quantum Dots in a Diblock Copolymer Matrix

by Frederick L. Beyer, Christopher R. Ziegler, Kevin Sill, Todd Emrick, Nicholas M. Benetatos, and Karen I. Winey

NOTICES

Disclaimers

The findings in this report are not to be construed as an official Department of the Army position unless so designated by other authorized documents.

Citation of manufacturer's or trade names does not constitute an official endorsement or approval of the use thereof.

Destroy this report when it is no longer needed. Do not return it to the originator.

Army Research Laboratory

Aberdeen Proving Ground, MD 21005-5069

ARL-TR-4204   **August 2007**

Directed Assembly of Quantum Dots in a Diblock Copolymer Matrix

Frederick L. Beyer and Christopher R. Ziegler
Weapons and Materials Research Directorate, ARL

Kevin Sill and Todd Emrick
University of Massachusetts Amherst

Nicholas M. Benetatos and Karen I. Winey
University of Pennsylvania

REPORT DOCUMENTATION PAGE

Form Approved
OMB No. 0704-0188

Public reporting burden for this collection of information is estimated to average 1 hour per response, including the time for reviewing instructions, searching existing data sources, gathering and maintaining the data needed, and completing and reviewing the collection information. Send comments regarding this burden estimate or any other aspect of this collection of information, including suggestions for reducing the burden, to Department of Defense, Washington Headquarters Services, Directorate for Information Operations and Reports (0704-0188), 1215 Jefferson Davis Highway, Suite 1204, Arlington, VA 22202-4302. Respondents should be aware that notwithstanding any other provision of law, no person shall be subject to any penalty for failing to comply with a collection of information if it does not display a currently valid OMB control number.
PLEASE DO NOT RETURN YOUR FORM TO THE ABOVE ADDRESS.

1. REPORT DATE (DD-MM-YYYY)	2. REPORT TYPE	3. DATES COVERED (From - To)
August 2007	Final	September 2004–August 2006

4. TITLE AND SUBTITLE	5a. CONTRACT NUMBER
Directed Assembly of Quantum Dots in a Diblock Copolymer Matrix	
	5b. GRANT NUMBER
	5c. PROGRAM ELEMENT NUMBER

6. AUTHOR(S)	5d. PROJECT NUMBER
Frederick L. Beyer, Christopher R. Ziegler, Kevin Sill,[*] Todd Emrick,[*] Nicholas M. Benetatos,[†] and Karen I. Winey[†]	AH-42
	5e. TASK NUMBER
	5f. WORK UNIT NUMBER

7. PERFORMING ORGANIZATION NAME(S) AND ADDRESS(ES)	8. PERFORMING ORGANIZATION REPORT NUMBER
U.S. Army Research Laboratory ATTN: AMSRD-ARL-WM-MA Aberdeen Proving Ground, MD 21005-5069	ARL-TR-4204

9. SPONSORING/MONITORING AGENCY NAME(S) AND ADDRESS(ES)	10. SPONSOR/MONITOR'S ACRONYM(S)
	11. SPONSOR/MONITOR'S REPORT NUMBER(S)

12. DISTRIBUTION/AVAILABILITY STATEMENT

Approved for public release; distribution is unlimited.

13. SUPPLEMENTARY NOTES

[*]Department of Polymer Science & Engineering, University of Massachusetts Amherst, Amherst, MA

[†]Department of Materials Science & Engineering, University of Pennsylvania, Philadelphia, PA

14. ABSTRACT

The effect of ligand molecular weight on nanoparticle dispersion and nanocomposite morphology has been investigated. Nanoscopic particles, CdSe/ZnS quantum dots (QDs), were dispersed into the polystyrene (PS) microdomains of a microphase separated, bulk PS-poly(methyl methacrylate) block copolymer. The QDs were compatibilized with the PS-domains of the microphase separated block copolymer by the use of PS-based ligands associated with the surfaces of the QDs. A stock solution of the functionalized particles was mixed with dissolved block copolymer, and bulk samples were formed by solvent evaporation. Dispersion of the nanoparticles was determined via bright field transmission election microscopy and high-angle annular dark field scanning transmission electron microscopy. The microphase separated block copolymer morphology (lamellae) was probed using small-angle and ultrasmall-angle x-ray scattering. Although the additive particles are much larger in diameter than those considered in previous calculations and experimental work, it was found that the QDs modified with 14,000 g/mol PS ligands dispersed well in the block copolymer, while those modified with 81,000 g/mol PS ligands formed small aggregates. In these nanoparticle/polymer composites, the block copolymer retains its original morphology.

15. SUBJECT TERMS

directed, assembly, quantum dot, HAADF, STEM, SAXS, block copolymer

16. SECURITY CLASSIFICATION OF:			17. LIMITATION OF ABSTRACT	18. NUMBER OF PAGES	19a. NAME OF RESPONSIBLE PERSON
a. REPORT	b. ABSTRACT	c. THIS PAGE			Frederick L. Beyer
UNCLASSIFIED	UNCLASSIFIED	UNCLASSIFIED	UL	20	19b. TELEPHONE NUMBER (Include area code) 410-306-0893

Standard Form 298 (Rev. 8/98)
Prescribed by ANSI Std. Z39.18

Contents

List of Figures

Acknowledgments

INTENTIONALLY LEFT BLANK.

1. Introduction

Dispersing nanoscopic particles in polymer matrices has become a topic of intense scientific and practical interest over the last two decades (*1–4*). The particles, matrices, and applications are greatly varied, including highly anisotropic clay platelets for improved mechanical and barrier properties, carbon nanotubes for electrical properties, and metallic nanoparticles for electro-optical applications. While some of these efforts have been very successful, in general, dispersing particles with a critical dimension on the order of a nanometer has proved challenging.

Theoretical results from Balazs and coworkers indicate that controlling parameters such as particle size and miscibility within a host material will allow manipulation of the preferred position of particles in a microphase separated diblock copolymer (*5–7*). For particles perfectly miscible within a copolymer microdomain, their results predict a relationship between microdomain size, given by the radius of gyration (R_g) of the overall block copolymer, and the size of the particle (R). Relatively large particles, where $R/R_g \geq 0.3$, were predicted to preferentially segregate to the centers of the microphase separated domains of the particular block in which they are miscible. Smaller particles, $R/R_g \leq 0.2$, are expected to segregate to the intermaterial dividing surfaces between microdomains. Such control of particle location, if feasible, could lead to a broad range of functional materials where value-added functionality is a result of both the nanoparticle properties and the organization of the particles on a nanometer length scale.

The basic tenets of these results have been shown to be reasonable in several systems. Bockstaller et al. (*8*) showed that large silica particles, where $R/R_g \approx 0.26$, preferentially segregated to the center of poly(ethylene-propylene) (PEP) domains in a lamellar poly(styrene)-*b*-PEP (PS-*b*-PEP) diblock copolymer. In contrast, 3.5-nm gold particles modified with C18 alkane ligands segregated to the edges of the PEP domain, presumably driven by the maximization of translational entropy for the small ($R/R_g \approx 0.06$) particles. Work by Kim et al. (*9*) demonstrated that the addition of a high volume fraction of nanoscopic particles can alter the morphological behavior of a diblock copolymer, PS-*b*-poly(2-vinylpyridene) (PS-*b*-P2VP). Addition of 2.5-nm-diameter gold nanoparticles, functionalized with short (1300 g/mol) thiol-terminated PS ligands, resulted in an ordered dispersion of the gold particles in the center of the PS domains at low loadings. In that case, R/R_g was ~0.24, calculated as $d/L \approx 5/21$, where d is the particle diameter and L is the domain period. At particle loadings of ~15 volume-percent, the lamellar morphology was not altered. Higher loadings of ~25 volume-percent particles produced a dramatic shift in the observed morphology, a logical result and in agreement with model predictions (*6*). A second study by Kim et al. (*10*) examined the effect on nanoparticle

dispersion of variations in the relative surface coverage by short thiol-terminated PS ligands (3400 g/mol), also in a PS-*b*-P2VP matrix. As a result of the inherent, although slight, attraction between Au nanoparticles and P2VP, it was shown that lowering the coverage of the particle surfaces with the PS ligands below 1.3 chains/nm^2 resulted in the particles localizing at the intermaterial dividing surfaces between microphase separated PS and P2VP domains. Finally, work by Lin et al. (*11*) examined the self-assembly of cadmium selenide (CdSe) and ferritin nanoparticles in a spin coated thin film of PS-*b*-P2VP. In that case, the particles were stabilized with tri-*n*-octylphosphine oxide (TOPO) ligands. When thin films were prepared from solutions containing both the particles and the matrix polymer, the TOPO-CdSe particles segregated to the P2VP domains, resulting in a pronounced change in the morphological behavior of the thin films.

In the present work, the bulk morphology of block copolymer/nanoparticle composites has been investigated. Here, CdSe quantum dots have been dispersed in a model block copolymer and the effects of ligand molecular weight on morphological behavior investigated for relatively high molecular weight ligands. The matrix material has been chosen so that a well-defined matrix morphology allows clear imaging of the effects of adding nanoparticles. Small-angle x-ray scattering (SAXS) and transmission electron microscopy (TEM) techniques have been used to determine the morphology of the bulk nanocomposite samples.

2. Experimental

CdSe/ZnS core-shell nanoparticles were synthesized by known methods, producing quantum dots of 3–4 nm diameter stabilized by TOPO ligands. These CdSe/ZnS nanoparticles were functionalized with a nitroxide-containing phosphine-oxide ligand that allowed polymerization from the nanoparticle surface by controlled free-radical polymerization (*12*). The molecular weight of the PS ligands was then determined by their removal from the particle surface and evaluation by gel permeation chromatography (GPC). Two different PS-functionalized nanoparticles were prepared, with PS ligands having number average molecular weights (M_n) of 14,000 g/mol and 81,000 g/mol.

The PS-*b*-PMMA diblock copolymer (Polymer Source, Inc., Canada) was used as received. The PS block has a M_n of 85,000 g/mol, the PMMA block has a M_n of 91,000 g/mol, and the polydispersity index of the copolymer was 1.12. The block copolymer was dissolved in toluene to form a dilute solution of ~2.5 weight-percent polymer. A small amount of a stock solution of the nanoparticles in toluene was added to the block copolymer solution so that the nanoparticles would comprise ~5 weight-percent of the final material. The solvent was allowed to evaporate slowly over a period of two weeks, after which the bulk samples were annealed under vacuum for 48 hr at 130 °C.

Thin sections of this composite material were prepared for electron microscopy by ultramicrotomy using a Leica UCT microtome and a diamond knife. The sections were ~50 nm thick. Bright field TEM was performed using a JEOL 200CX operated at 120 kV accelerating voltage. HAADF STEM experiments were performed on a JEOL 2010F field emission electron microscope operated at 197 kV with a 70-µm condenser aperture. Images (512×512 pixels) were acquired using a Gatan HAADF scintillating detector with linear intensity response and collection angle ranging between 50 and 115 mRAD. For presentation, post-analysis image enhancement was performed with Photoshop[*] 5.0 using standard techniques, including gray-level adjustment and brightness/contrast manipulation. These adjustments were applied uniformly to entire images.

SAXS data were collected using a pinhole collimated instrument with an approximate sample-detector distance of 1.1 m and $Cu_{K\alpha}$ ($\lambda = 1.542$ Å) x-rays generated at 2.4 kW with a Rigaku Ultrax18 rotating anode source. Two-dimensional (2-D) data sets were collected using a Molecular Metrology multi-wire detector, then corrected for background scattering and scaled to absolute intensity using a previously calibrated type-2 glassy carbon standard. The 2-D data sets were then azimuthally averaged giving intensity, $I(q)$, where q is the magnitude of the scattering vector, given by $q = 4\pi \cdot \sin(\theta)/\lambda$, with scattering angle 2θ.

Ultrasmall-angle x-ray scattering (USAXS) data were collected at a wavelength of $\lambda = 1.0256$ Å (12.1 keV) on the Bonse-Hart USAXS instrument, located at the UNICAT beamline 33-ID at the Advanced Photon Source of the Argonne National Laboratory. USAXS data, also reported as intensity as a function of scattering vector, were corrected for background scattering. Although the USAXS instrument is slit-collimated and thus smears the data, the smeared data are presented here due to the distortion of Bragg diffraction peaks by desmearing algorithms. All USAXS and SAXS data correction and analysis were performed using Wavemetrics IGOR Pro 5.04B and procedures written by Dr. Jan Ilavsky of the Argonne National Laboratory.

3. Results and Discussion

Figure 1 shows a representative HAADF STEM micrograph of the bulk PS-*b*-PMMA diblock copolymer containing CdSe/ZnS quantum dots. Dispersion of the QDs was achieved via surface modification with 14,000 g/mol PS ligands. The technique of HAADF STEM provides imaging in which contrast is generated by differences in local average atomic number (Z). When an area of increased local average Z is encountered by the convergent beam, the electrons are elastically scattered to high angles and are detected. Thus, HAADF STEM images depict areas of increased average atomic number as bright regions amidst a dark background because electrons scattered at small angles (i.e., by lower Z regions) pass through the annular detector. The lamellar

---

[*]Photoshop is a registered trademark of Adobe Systems, Inc., San Jose, CA.
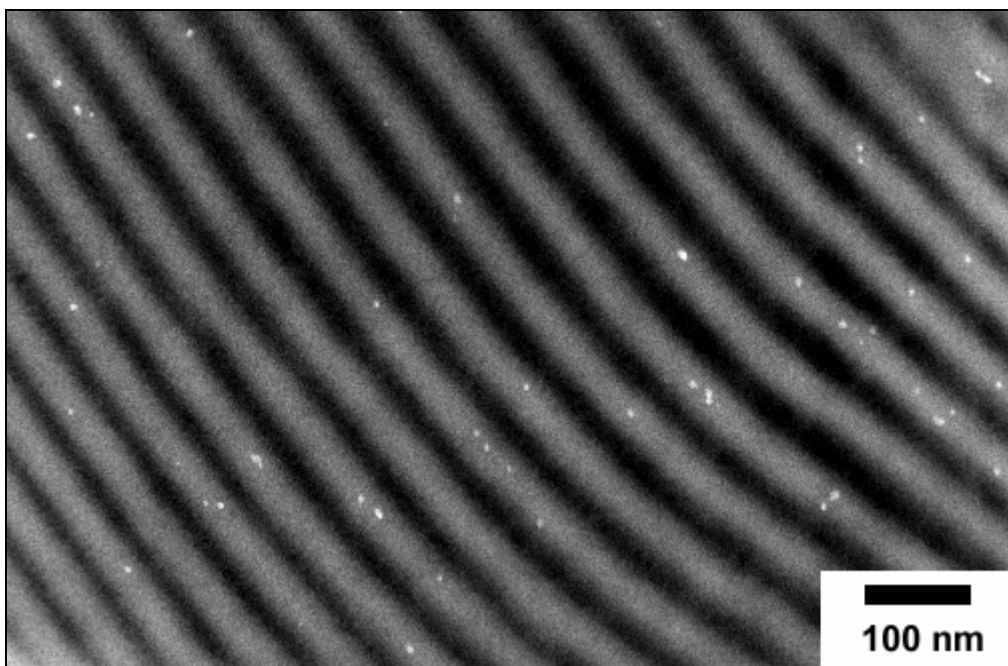
Figure 1. High-angle annular dark field (HAADF) STEM micrograph showing the lamellar morphology of the PS-*b*-PMMA block copolymer and CdSe/ZnS quantum dots with 14,000 g/mol ligand dispersed in the PS (light) domains.

morphology of the PS-*b*-PMMA diblock copolymer matrix is clearly visible, with alternating PS domains (light) and PMMA domains (dark). Since electron irradiation degrades the PMMA microdomains more severely than PS, these thinner, less dense areas produce less elastic scattering and the PMMA microdomains appear dark. The nanoparticles, which have significantly higher average Z relative to the diblock copolymer matrix, appear clearly as bright spots. The lamellar period can be estimated based on the micrograph to be ~63 nm. In figure 2, it is clear that the nanoparticles are preferentially dispersed in the PS domains, a direct result of the selective miscibility of the ligands used to functionalize the particle surfaces. Very few nanoparticles were observed in the PMMA domains.

A representative bright field TEM micrograph of the bulk PS-*b*-PMMA copolymer containing QDs modified with 81,000 g/mol PS ligands is shown in figure 3. Contrast in bright field TEM also derives from variations in electron density. Electrons that interact with electron-rich regions of the sample are scattered to high angles and away from the imaging media, resulting in contrast opposite of that in dark field mode. In figure 3, the majority of QDs are observed in small agglomerates (dark), although these agglomerates generally were found in the PS domains of the microphase separated block copolymer. In general, few if any isolated particles were observed for QDs modified with the higher molecular weight ligand.

The SAXS and USAXS data, figure 4, confirm that the lamellar morphology of the neat block copolymer was not altered significantly by the addition of 5 weight-percent QDs. The SAXS data show complete Bragg diffraction peaks centered at $q_3 = 0.030$ Å^{-1} and $q_5 = 0.050$ Å^{-1}. For
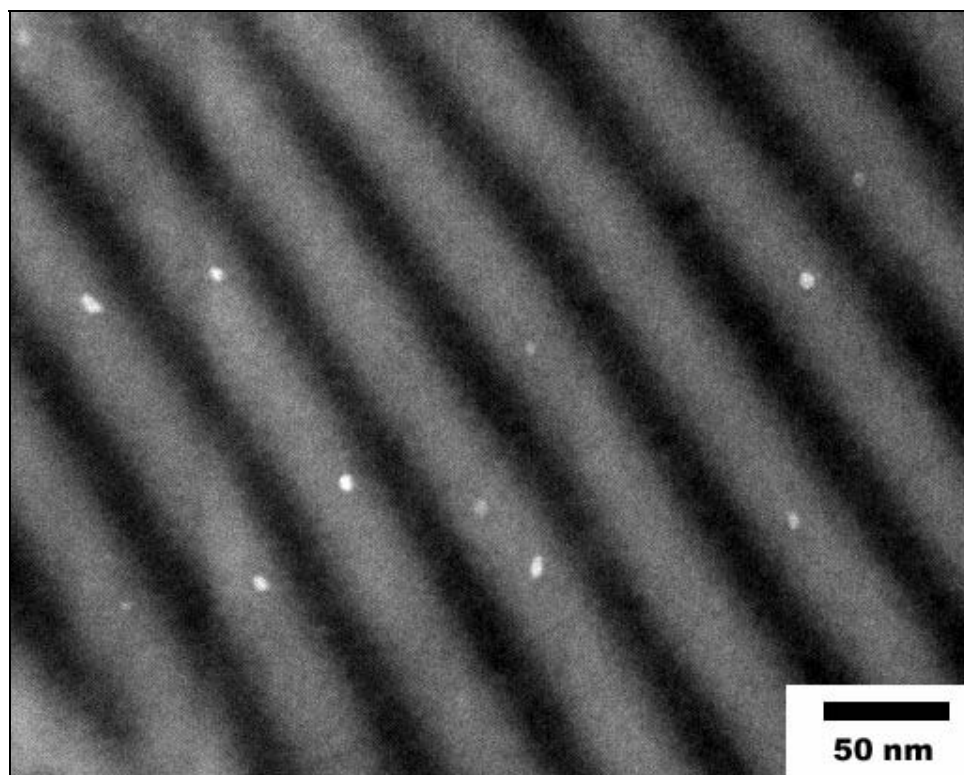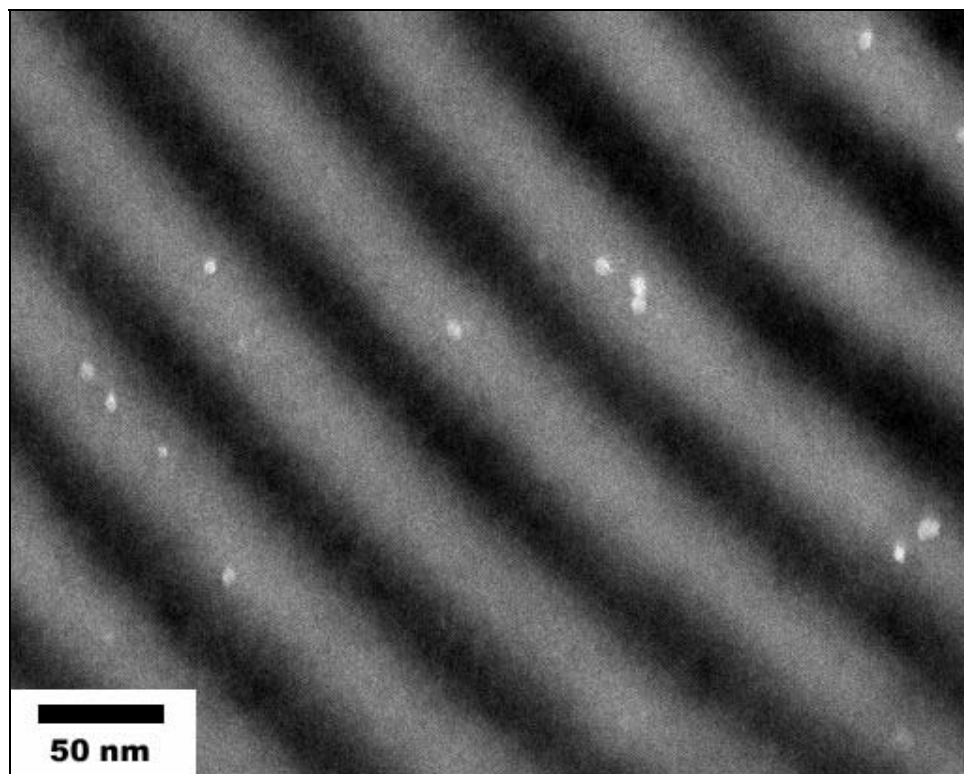
Figure 2. HAADF STEM micrographs illustrating the preferential exclusion of
  CdSe/ZnS quantum dots with 14,000 g/mol ligands from the PMMA (dark)
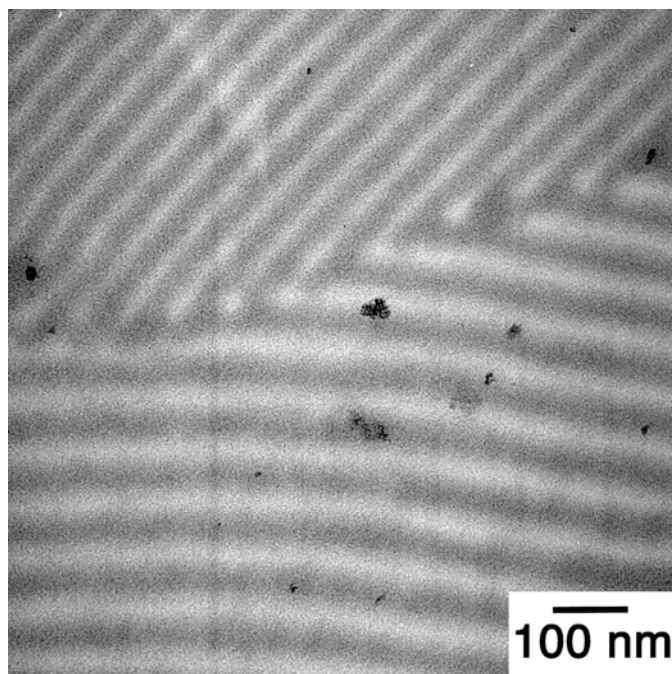 microdomains of the block copolymer.

Figure 3. Bright field TEM micrograph showing small aggregates (dark) of CdSe/ZnS quantum dots with 81,000 g/mol ligands in the PS-*b*-PMMA copolymer matrix. The large MW of the ligand makes dispersion of the nanoparticles more difficult by effectively increasing particle diameter.

the neat block copolymer, a third complete Bragg diffraction peak is observed at $q_7 = 0.071$ Å^{-1}. From symmetry operations, a lamellar morphology gives rise to Bragg reflections which occur at values of q that are integer multiples of the q-value for the primary peak, q^*. The USAXS data indicate that the primary Bragg reflection for the neat block copolymer sample lies at $\sim q^*$ $= 0.010$ Å^{-1}, corresponding to a lamellar period of 63 nm. The absence of the even multiple Bragg reflections (q_2, q_4, and q_6) arises from the nearly equal thicknesses of the PS and PMMA domains (*13*). The SAXS and USAXS data both show fewer Bragg peaks for the samples containing the nanoparticles, indicating a slight decrease in long-range order in those samples. No upturn is observed at the lowest regions of the USAXS data, indicating that, if larger particle agglomerates are present in the sample, they are macroscopic in size (*14*).

These findings agree with reported results for relatively large diameter nanoparticles dispersed in block copolymers and with the mean field model predictions. For large particles, where R/R$_g$ (or particle diameter, d, divided by domain thickness, L) greater than ~0.25, the need to minimize the entropic effects of chain stretching outweigh the entropic benefits of mixing and thereby drives the particles to the center of the block copolymer microdomains in which they are miscible. Here, even though the CdSe/ZnS particle diameters are small (3.5 nm), the addition of the PS ligands increases the effective size of the particle significantly. For the shorter ligand, this effective particle size is estimated to be 19.3 nm, the sum of the 3.5 nm CdSe/ZnS core
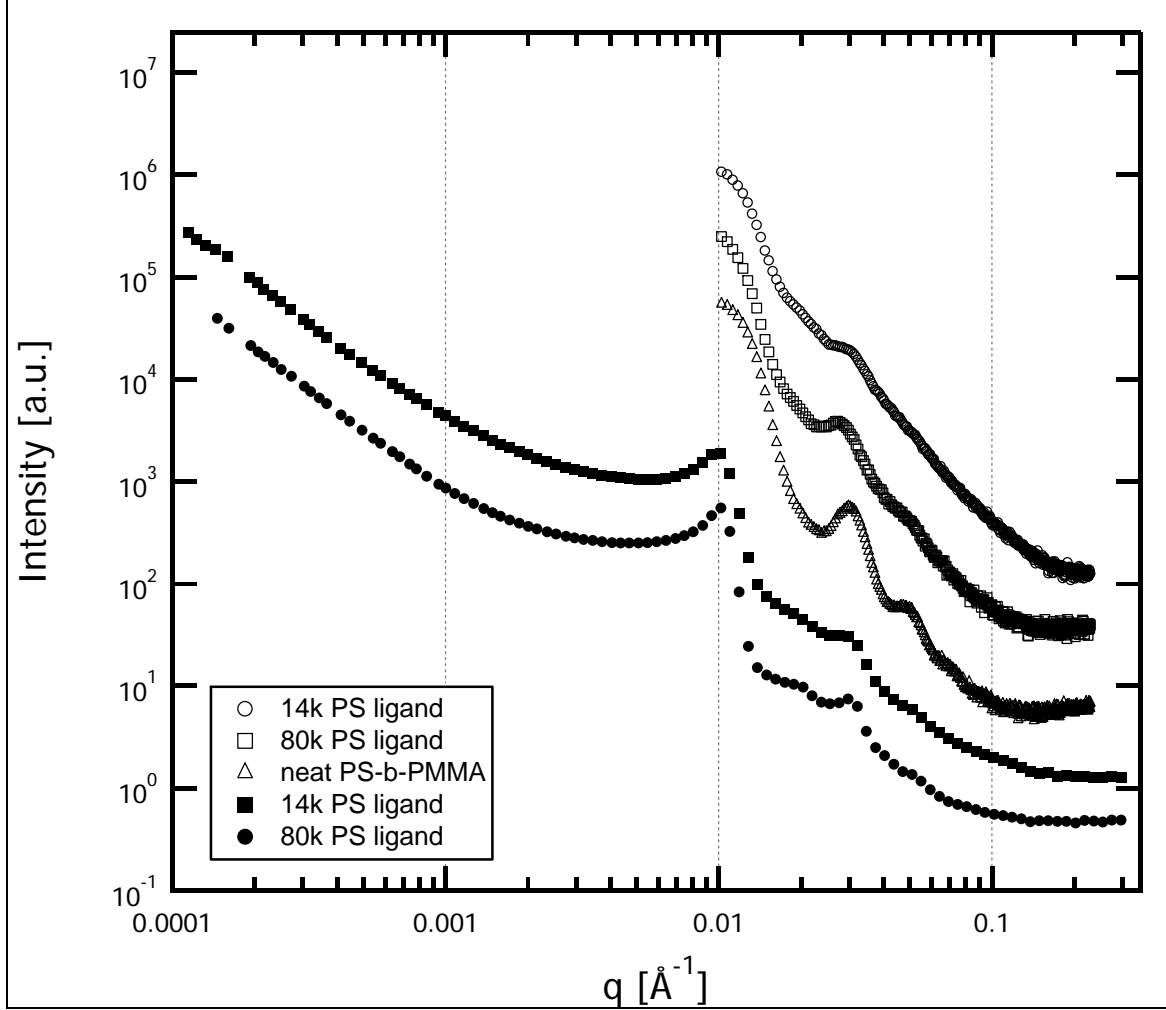
Figure 4. SAXS (open) and USAXS (filled) data for both neat PS-*b*-PMMA block copolymer and block
copolymer with dispersed CdSe/ZnS quantum dots. All data have been scaled vertically for
clarity.

diameter and twice the R_g of a 14,000 g/mol PS molecule (7.9 nm). From the SAXS data, the PS
domain dimension is estimated to be approximately 35 nm. This gives a d/L ratio of ~0.55, well
above the value used by Balazs and coworkers. The dispersion of such large particles in block
copolymers illustrates the importance of the enthalpic interactions in determining the
morphology of these composite materials. The observed morphological behavior of the sample
with the longer, 81,000 g/mol ligands would seem to provide an empirical upper bound to the
length of the ligand that should be used to disperse a particle. In that case, the ligand radius of
gyration is roughly 19 nm, making the effective particle size ~42 nm. Here the effective particle
size is greater than the PS domain and far outside the limits considered by Balazs and coworkers.
The lack of single, dispersed nanoparticles in favor of small clusters indicates that, perhaps even
in solution, aggregation is favored when the nanoparticles are modified with a long ligand.

4. Conclusions

Nanoscopic quantum dots of CdSe with shells of ZnS were functionalized with PS ligands and dispersed in a bulk PS-*b*-PMMA copolymer. Two relatively high ligand molecular weights, 14,000 g/mol and 81,000 g/mol, resulted in dramatically different behaviors. Particles modified with the 14,000 g/mol ligand dispersed in the PS lamellae of the microphase separated block copolymer, while those modified with the higher molecular weight ligand were found almost exclusively in small aggregates. In both cases, the effective diameter of the particle (including ligands) was greater than that considered in previous calculations, and the dispersion of nanoparticles with R/R_g ratios as high as 0.55 illustrates the importance of enthalpic interactions on morphological behavior in such nanoparticle/polymer composites.

5. References

1. Pinnavaia, T. J.; Beall, G. W., Eds. *Polymer-Clay Nanocomposites*; John Wiley & Sons: New York, 2000.

2. Shenhar, R.; Norsten, T. B.; Rotello, V. M. *Adv. Mater.* **2005**, *17*, 657–669.

3. Bockstaller, M. R.; Mickiewicz, R. A.; Thomas, E. L. *Adv. Mater.* **2005**, *17*, 1331–1349.

4. Moniruzzaman, M.; Winey, K. I. *Macromolecules* **2006**, *39*, 5194–5205.

5. Thompson, R. B.; Ginzburg, V. V.; Matsen, M. W.; Balazs, A. C. *Science* **2001**, *292*, 2469–2472.

6. Lee, J. Y.; Thompson, R. B.; Jasnow, D.; Balazs, A. C. *Macromolecules* **2002**, *35*, 4855–4858.

7. Lee, J. Y.; Thompson, R. B.; Jasnow, D.; Balazs, A. C. *Faraday Discuss.* **2003**, *123*, 121–131.

8. Bockstaller, M. R.; Lapetnikov, Y.; Margel, S.; Thomas, E. L. *J. Am. Chem. Soc.* **2003**, *125*, 5276–5277.

9. Kim, B. J.; Chiu, J. J.; Yi, G. R.; Pine, D. J.; Kramer, E. J. *Adv. Mater.* **2005**, *17*, 2618–2622.

10. Kim, B. J.; Bang, J.; Hawker, C. J.; Kramer, E. J. *Macromolecules* **2006**, *39*, 4108–4114.

11. Lin, Y.; Boker, A.; He, J. B.; Sill, K.; Xiang, H. Q.; Abetz, C.; Li, X. F.; Wang, J.; Emrick, T.; Long, S.; Wang, Q.; Balazs, A.; Russell, T. P. *Nature* **2005**, *434*, 55–59.

12. Sill, K.; Emrick, T. *Chemistry of Materials* **2004**, *16*, 1240–1243.

13. Roe, R. -J. *Methods of X-ray and Neutron Scattering in Polymer Science*; Oxford University Press: New York, 2000.

14. Kammler, H. K.; Beaucage, G.; Mueller, R.; Pratsinis, S. E. *Langmuir* **2004**, *20*, 1915–1921.

NO. OF
COPIES ORGANIZATION

<u>ABERDEEN PROVING GROUND</u>

1   DIR USARL
       AMSRD ARL WM MA
         F BEYER

INTENTIONALLY LEFT BLANK.